Nonlinear torsional wave propagation in cylindrical coordinates to assess biomechanical parameters.

J. Naranjo-Pérez[1], M. Riveiro[2], A. Callejas[2], G. Rus[2,3,4], and J. Melchor[2,3,4]

[1]Department of Continuum Mechanics and Structural Analysis, Universidad de Sevilla, Seville, Spain
[2]Department of Structural Mechanics, University of Granada, Granada, Spain
[3]Biosanitary Research Institute, Granada, Spain
[4]Excellence Research Unit "Modelling Nature" (MNat) University of Granada, Granada, Spain

Abstract

A formulation in cylindrical coordinates of the nonlinear torsional wave propagation on a hyperelastic material characterized by Hamilton's strain energy function is proposed. The objective of this formulation is to study and assess soft tissues, taking into account both geometrical and physical nonlinearity. Specifically, this work analyzes the propagation of torsional shear waves through an isotropic axisymmetric medium, so the only non-zero velocity component is associated with the angular coordinate. To transform the equations from Cartesian to cylindrical coordinates, the covariant and contravariant transformations are employed.

A transverse torsional wave propagating through a quasi-incompressible hydrogel from the emitter to the receiver is considered. As the close form solution is not straightforward, a numerical simulation using the Finite Difference Time Domain method is performed. The results are obtained for a realistic range of wave frequencies and nonlinear parameters for medical applications.

1 Introduction

Linear elasticity is a simplified version of nonlinear elasticity, which is valid for certain problems where nonlinear terms are negligible. Geometrical nonlinearity is useful when the strains of the deformable solid subjected to external stresses are no longer small, these terms become relevant and the linear theory is not valid. Additionally, the physical or constitutive nonlinearity associated with the material properties arises when the relationship between stresses and strains is not linear. For the purpose of correctly developing this formulation, both nonlinearities must be considered.

Landau and Lifshitz proposed in one exercise in 1956 to obtain nonlinear motion equations from the relation between the internal elastic energy function and the stress tensor [?]. Goldberg in 1961 and Zarembo in 1966 solved in parallel the problem defining a strain energy function [?, ?]. Afterwards, the Third Order Elastic Constants (TOEC) were formulated and the invariants of the Green-Lagrange strain tensor defined by Eringen *et al.* in 1974 [?].

Zarembo was first to measure experimentally in 1971 the TOEC for some metals and crystals [?]. In 1988, Hamilton obtained the experimental B/A parameter for liquids and tissues [?]. Hamilton and Zabolotskaya, motivated by the work of Catheline *et al.* [?] who measured the TOEC proposed by Landau and Lifshitz, presented a new formulation of the fourth order strain energy function for an isotropic medium [?]. In case of tissue-like media, it is practically incompressible and the strain energy function may be simplified. Destrade and Ogden in 2010 expanded to the fourth order Landau's strain energy function and determined the exact behavior of the second, third and fourth order elastic constants in the incompressible limit of isotropic materials using the logarithmic strain measure [?].

The nonlinear elastic theory has aroused a huge interest in the study of nonlinear materials, including hard and soft tissues [?, ?, ?, ?]. The investigation in shear and longitudinal waves propagation in soft tissues began in 1952 in hand of Henning von Gierke [?]. The ultrasonic imaging in soft tissues started in the 80s decade when Fujimoto *et al.* described the use of dynamic tests to ultrasonically estimate the compressibility and mobility of breast tumors [?].

Ultrasonic shear waves have been used by many authors in order to measure the linear and nonlinear elastic properties of hyperelastic materials such as tissues. The Static Elastography, originally proposed by Ophir *et al.* [?], has been successfully used to measure nonlinear properties of vascular tissues or malingnant and beningn tumors of breast tissues [?, ?, ?, ?]. Nevertheless, the results of this method are not satisfactory for organs or tissues which are deep or difficult to compress as the strain profile may be uncertain. The Transient Elastography introduced by Stefan Catheline [?] has been used, for example, to diagnose cirrhosis [?] and for assessment of hepatic fibrosis [?]. The Supersonic Shear Imaging (SSI) technique, presented in 2004 by Bercoff and Tanter [?], has also been used to obtain the third and fourth order constants, A and D, respectively, of pig brain tissue or human breast tissue. However, these studies were limited to *ex vivo* experiments [?, ?, ?].

Recent research focuses on the propagation of torsional waves due to the limitations of shear and compressional waves [?]. First, this type of wave can propagate by quasi-fluids media and, since it propagates at the S-wave speed c_s, it is more sensitive to consistency changes caused, for example, by tumors [?, ?]. Second, the variations of mechanical parameters are more sensitive in the regime of low energy where this wave is generated. Finally, torsional movement does not generate secondary interfering P-waves at the boundary of the transducer where pure shear waves are difficult to create [?, ?]. A torsional ultrasonic transducer has been used to measure nonlinear parameters of ligament tissue and the shear modulus of cervical tissue in pregnant women [?, ?]. These results and prospects justify the selection of torsional waves in this study for nonlinear soft tissue analysis.

The goal of this paper is to elaborate a new formulation in cylindrical coordinates of a nonlinear torsional wave propagating on a hyperelastic material defined by the Hamilton's strain energy function. While the quadratically nonlinear propagation of the torsional wave on a hyperelastic material has been studied [?], the consideration of all nonlinear terms in the equations has not, to our knowledge, yet been included. By considering all nonlinear terms allows to understand the behavior of the material in a more reliable way.

As the nonlinear equations obtained are complex, numerical techniques must be used to solve them. In particular, the Finite Difference Time Domain (FDTD) method is used in the numerical simulations [?]. As a result, the displacement is obtained for both realistic ranges of torsional wave frequencies and nonlinear constants of the hyperelastic tissue-like material for medical applications.

2 Theoretical background

The Green-Lagrange strain tensor that governs the elasticity is defined in index notation as,

$$\varepsilon_{ij} = \frac{1}{2}(u_{i,j} + u_{j,i} + u_{l,i}u_{l,j}) \tag{1}$$

where the third term in Equation 1 is related with geometrical nonlinearity. The physical nonlinearity is here focused on hyperelastic materials, in which the strain energy function $\mathcal{W}$ is defined per unit reference (undeformed) volume and acts as potential of the stress.

The strain energy function is defined following the expression by Landau and Lifshitz [?],

$$\mathcal{W} = \frac{\lambda}{2}I_1^2 + \mu I_2 + \frac{A}{3}I_3 + BI_1I_2 + \frac{C}{3}I_1^3 \tag{2}$$

where μ and λ are the Lamé constants and A, B and C are the TOEC. I_1, I_2 and I_3 are the invariants of the Green-Lagrange strain tensor defined by Eringen *et al.* in 1974 [?],

$$\begin{aligned} I_1 = &\quad \operatorname{tr}\boldsymbol{\varepsilon} &&= \varepsilon_{ii} \\ I_2 = &\quad \operatorname{tr}\boldsymbol{\varepsilon}^2 &&= \varepsilon_{ij}\varepsilon_{ji} \\ I_3 = &\quad \operatorname{tr}\boldsymbol{\varepsilon}^3 &&= \varepsilon_{ij}\varepsilon_{jl}\varepsilon_{li} \end{aligned} \tag{3}$$

The expansion to fourth order of the energy density is necessary when the nonlinear effects in shear waves are considered. This is because for incompressible media, nonlinearity at third order is missing in the particle displacement [?]. This expansion is characterized by four new terms, yielding,

$$\mathcal{W} = \frac{\lambda}{2}I_1^2 + \mu I_2 + \frac{A}{3}I_3 + BI_1I_2 + \frac{C}{3}I_1^3 + DI_2^2 + EI_1I_2 + FI_1^2I_2 + GI_1^4 \tag{4}$$

where D, E, F and G are the Fourth Order Elastic Constants (FOEC).

When the case of quasi-incompressible soft tissue media is analyzed, where $\lambda >> \mu$, the strain energy function is simplified to,

$$\mathcal{W} = \mu I_2 + \frac{1}{3}AI_3 + DI_2^2 \tag{5}$$

where A and D are the third and fourth order elastic constants, respectively [?].

2.1 Nonlinear torsional waves in isotropic cylindrical coordinates

This paper focuses on the analysis of a transverse torsional wave propagating along an isotropic cylindrical reference system. This problem is expected to be expressed in cylindrical coordinates because of the following reason. As the OZ axis is an axis of symmetry, this configuration is axilsymmetric. Hence, deriving the formulation in cylindrical coordinates has the advantage of solving 3D problems by 2D equations. In this case, the configuration only depends on the velocity of the angular coordinate θ, and the velocity in the two others components are negligible [?]. For the mathematical derivation, the covariant and contravariant coordinates are used. The use of these coordinates is justified for simplifying the formulation. In this manner, the transformation of the momentum equation from the Cartesian coordinate system to the cylindrical coordinate system is carried out in a more straightforward way.

The covariant basis, denoted as $\mathbf{g}_i$, and the contravariant basis, $\mathbf{g}^i$, for the cylindrical coordinate system, can be calculated using the following expressions,

$$\mathbf{g}_i = \frac{\partial x^1}{\partial \xi^i}\mathbf{e}_1 + \frac{\partial x^2}{\partial \xi^i}\mathbf{e}_2 + \frac{\partial x^3}{\partial \xi^i}\mathbf{e}_3 \tag{6}$$

$$\mathbf{g}^i = \frac{\partial \xi^i}{\partial x^1}\mathbf{e}^1 + \frac{\partial \xi^i}{\partial x^2}\mathbf{e}^2 + \frac{\partial \xi^i}{\partial x^3}\mathbf{e}^3 \tag{7}$$

where ξ^i is the cylindrical coordinate i and x^1, x^2, x^3 are the Cartesian coordinates with fixed orthonormal base vectors $\mathbf{e}^1$, $\mathbf{e}^2$, $\mathbf{e}^3$, respectively. The two coordinate systems are related according to,

$$\xi^1 = r = \sqrt{(x^1)^2 + (x^2)^2} \tag{8}$$

$$\xi^2 = \theta = \arctan\frac{x^2}{x^1} \tag{9}$$

$$\xi^3 = z = x^3 \tag{10}$$

$$x^1 = r\cos\theta \tag{11}$$

$$x^2 = r\sin\theta \tag{12}$$

$$x^3 = z \tag{13}$$

By substituting Equations 8-13 into Equations 6 and 7,

$$\begin{aligned}
\mathbf{g}_1 &= \frac{\partial x^1}{\partial \xi^1}\mathbf{e}_1 + \frac{\partial x^2}{\partial \xi^1}\mathbf{e}_2 + \frac{\partial x^3}{\partial \xi^1}\mathbf{e}_3 = \cos\theta\mathbf{e}_1 + \sin\theta\mathbf{e}_2 + 0\mathbf{e}_3\\
\mathbf{g}_2 &= \frac{\partial x^1}{\partial \xi^2}\mathbf{e}_1 + \frac{\partial x^2}{\partial \xi^2}\mathbf{e}_2 + \frac{\partial x^3}{\partial \xi^2}\mathbf{e}_3 = -r\sin\theta\mathbf{e}_1 + r\cos\theta\mathbf{e}_2 + 0\mathbf{e}_3\\
\mathbf{g}_3 &= \frac{\partial x^1}{\partial \xi^3}\mathbf{e}_1 + \frac{\partial x^2}{\partial \xi^3}\mathbf{e}_2 + \frac{\partial x^3}{\partial \xi^3}\mathbf{e}_3 = 0\mathbf{e}_1 + 0\mathbf{e}_2 + 1\mathbf{e}_3
\end{aligned} \tag{14}$$

and,

$$\begin{aligned}
\mathbf{g}^1 &= \frac{\partial \xi^1}{\partial x^1}\mathbf{e}^1 + \frac{\partial \xi^1}{\partial x^2}\mathbf{e}^2 + \frac{\partial \xi^1}{\partial x^3}\mathbf{e}^3 = \frac{x^1}{r}\mathbf{e}^1 + \frac{x^2}{r}\mathbf{e}^2 + 0\mathbf{e}^3\\
\mathbf{g}^2 &= \frac{\partial \xi^2}{\partial x^1}\mathbf{e}^1 + \frac{\partial \xi^2}{\partial x^2}\mathbf{e}^2 + \frac{\partial \xi^2}{\partial x^3}\mathbf{e}^3 = -\frac{x^2}{r^2}\mathbf{e}^1 + \frac{x^1}{r^2}\mathbf{e}^2 + 0\mathbf{e}^3\\
\mathbf{g}^3 &= \frac{\partial \xi^3}{\partial x^1}\mathbf{e}^1 + \frac{\partial \xi^3}{\partial x^2}\mathbf{e}^2 + \frac{\partial \xi^3}{\partial x^3}\mathbf{e}^3 = 0\mathbf{e}^1 + 0\mathbf{e}^2 + 1\mathbf{e}^3
\end{aligned} \tag{15}$$

The metric tensor is obtained as the dot product of the covariant and the contravariant base vectors. For the cylindrical coordinate system, the covariant and the contravariant components of the metric tensor are defined in Equations 16 and 17, respectively.

$$g_{ij} = g_i \cdot g_j = \begin{bmatrix} 1 & 0 & 0 \\ 0 & r^2 & 0 \\ 0 & 0 & 1 \end{bmatrix} \tag{16}$$

$$g^{ij} = g^i \cdot g^j = \begin{bmatrix} 1 & 0 & 0 \\ 0 & \frac{1}{r^2} & 0 \\ 0 & 0 & 1 \end{bmatrix} \tag{17}$$

The Christoffel symbols of the second kind represent the coefficients of the Levi-Civita connection [?]. Since this connection has zero torsion, the Christoffel symbols are symmetric relative to the lower indices, i.e., $\Gamma^k_{ij} = \Gamma^k_{ji}$. In cylindrical coordinates, the only non-zero Christoffel symbols are given in Equations 18 and 19 [?],

$$\Gamma^1_{22} = -r \tag{18}$$

$$\Gamma^2_{12} = \Gamma^2_{21} = \frac{1}{r} \tag{19}$$

Using the above formulation, the strain tensor of the benchmark problem can be derived. For this purpose, first, the expression of the displacements is obtained. The covariant components of the displacement vector are,

$$u_1 = u_r = 0 \qquad u_2 = r u_\theta(r,z) \qquad u_3 = u_z = 0 \tag{20}$$

and the contravariant components,

$$u^1 = u_r = 0 \qquad u^2 = \frac{1}{r} u_\theta(r,z) \qquad u^3 = u_z = 0 \tag{21}$$

being u_θ the angular displacement. The Green-Lagrange strain tensor of Equation 1 can be evaluated using the covariant derivatives of the covariant and contravariant components of the displacement vector, according to the expression [?],

$$\varepsilon_{ij} = \frac{1}{2}\left[\nabla_i u_j + \nabla_j u_i + \nabla_i u_k \nabla_j u^k\right] \tag{22}$$

where the covariant derivative of the covariant components and the covariant derivative of the contravariant components are computed following the Equations 23 and 24 respectively [?],

$$\nabla_i u_j = \frac{\partial u_j}{\partial \xi^i} - u_k \Gamma^k_{ji} \tag{23}$$

$$\nabla_i u^k = \frac{\partial u^k}{\partial \xi^i} + u^j \Gamma^k_{ji} \tag{24}$$

The Green-Lagrange strain tensor in cylindrical coordinates is obtained by replacing the displacements (Equations 20-21) into the Equation 22. This tensor is defined with respect to the undeformed position vector coordinates, so-called Lagrangian coordinate. The Green-Langrange strain tensor has the following expression,

$$\varepsilon_{ij} = \begin{bmatrix} \frac{1}{2}u^2_{\theta,r} & \frac{1}{2}(r u_{\theta,r} - u_\theta) & \frac{1}{2}u_{\theta,r}u_{\theta,z} \\ \frac{1}{2}(r u_{\theta,r} - u_\theta) & \frac{1}{2}u^2_\theta & \frac{1}{2} r u_{\theta,z} \\ \frac{1}{2}u_{\theta,r}u_{\theta,z} & \frac{1}{2} r u_{\theta,z} & \frac{1}{2}u^2_{\theta,z} \end{bmatrix} \tag{25}$$

3 Motion equation for the nonlinear torsional wave

Since the Green-Lagrange strain tensor is defined in the Lagrangian configuration, the stress tensor used to define the constituve equation must also be defined in Lagrangian coordinates. In this study, the *second Piola-Kirchhoff* stress tensor, $\mathcal{S}$, is considered for this purpose. The constitutive equation allows obtaining the stresses as a function of the displacements. Introducing them into the momentum equation gives as result the balance of momentum equation written in terms of the displacements. The starting point is the momentum equation in Lagrangian coordinates, which is defined as follows [?],

$$\rho\frac{\partial \mathbf{v}}{\partial t} = \rho\mathbf{g} + \nabla\cdot\boldsymbol{\mathcal{T}}^T \tag{26}$$

where $\frac{\partial \mathbf{v}}{\partial t}$ is the acceleration in the Lagrangian configuration, ρ is the density, $\mathbf{g}$ are the body forces and $\boldsymbol{\mathcal{T}}$ is the *first Piola-Kirchhoff* stress tensor. This equation can be rewritten in index notation as follows, where upper case indices have been considered to refer to an orthonormal base,

$$\rho\frac{\partial^2 u_J}{\partial t^2} = \rho g_J + \frac{\partial \mathcal{T}_{IJ}}{\partial X_I} \tag{27}$$

where X_I denotes the Lagrangian coordinate I. The main drawback of the first Piola-Kirchhoff stress tensor, $\mathcal{T}$, is that it is not symmetric.

To restore the symmetry, the *second Piola-Kirchhoff* stress tensor, $\mathcal{S}$, is introduced as,

$$\mathcal{S}_{IJ} = F^{-1}_{IK}\mathcal{T}_{KJ} = \det(F)F^{-1}_{IK}\sigma_{KP}F^{-1}_{JP} \tag{28}$$

where F is the deformation gradient, which is defined as $F_{IJ} = \frac{\partial x_I}{\partial X_J}$ and σ_{KP} is the Cauchy stress tensor.

The covariant and contravariant components are introduced herein to simplify the following mathematical procedure. Neglecting volumetric forces, Equation 27 is expressed using the contravariant components of $\mathcal{T}$ as [?],

$$\rho\frac{\partial^2 u^k}{\partial t^2} = \nabla_i\mathcal{T}^{ik} \tag{29}$$

where $\nabla_i\mathcal{T}^{ik}$ is the divergence of the first Piola-Kirchhoff written in index notation. From Equation 28, the first and the second Piola-Kirchhoff stress tensors are related in terms of the contravariant components via the following equation,

$$\mathcal{T}^{ik} = F^i_j\mathcal{S}^{jk} = \left(\frac{\partial x^i}{\partial X_j}\right)\mathcal{S}^{jk} = \left(\frac{\partial (X^i+u^i)}{\partial X_j}\right)\mathcal{S}^{jk} = \left(\delta^i_j + \frac{\partial u^i}{\partial X_j}\right)\mathcal{S}^{jk} \tag{30}$$

By substituting the relation above into the Equation 29, the motion equation in the contravariant basis in the Lagrangian configuration is obtained,

$$\nabla_i\left[\left(\delta^i_j + \nabla_j u^i\right)\mathcal{S}^{jk}\right] = \rho\frac{\partial u^k}{\partial t^2} \tag{31}$$

This is the compact form of the momentum equation expressed in the Lagrangian configuration. To expand the equation, several previous steps are required. The covariant derivative of the contravariant components is calculated by using the Equation 24. The tensor including these derivatives multiplied by $\mathcal{S}^{jk}$ gives as a result another second kind tensor, $\nabla_j u^i \cdot \mathcal{S}^{jk} = \mathcal{C}^{ik}$. Hence, Equation 31 can be reformulated as the divergence of a tensor $\mathcal{B}^{ik}$, which results from adding the two previous tensors,

$$\begin{aligned}\nabla_i \left[\mathcal{S}^{ik} + \mathcal{C}^{ik}\right] &= \rho \frac{\partial u^k}{\partial t^2} \\ \nabla_i \mathcal{B}^{ik} &= \rho \frac{\partial u^k}{\partial t^2}\end{aligned} \tag{32}$$

where the divergence of the contravariant components of any tensor is calculated by,

$$\nabla_i \mathcal{B}^{ik} = \frac{\partial \mathcal{B}^{ik}}{\partial \xi^i} + \mathcal{B}^{mk}\Gamma^i_{mi} + \mathcal{B}^{im}\Gamma^k_{mi} \tag{33}$$

Therefore, Equation 32 may be expressed as:

$$\frac{\partial \mathcal{B}^{ik}}{\partial \xi^i} + \mathcal{B}^{mk}\Gamma^i_{mi} + \mathcal{B}^{im}\Gamma^k_{mi} = \rho \frac{\partial u^k}{\partial t^2} \tag{34}$$

Note that for this particular case, the general coordinates are $\xi^1 = r$, $\xi^2 = \theta$ and $\xi^3 = z$, the Christoffel symbols are zero except those in Equations 18-19 and the configuration depends only on the velocity of the angular coordinate θ. The summation rule is used here. Hence, the first term is decoupled in three summands and the second and the third term are decoupled in nine summands each. Equation 34 represents a set of equations, one per each value of the index $k = 1, 2, 3$. In the following, dots denote derivatives with respect to time. [redacted]

$$\begin{aligned}&(\mathcal{S}^{12})_{,r} + (\mathcal{S}^{23})_{,z} + \frac{1}{r}\left(\mathcal{S}^{12} - \mathcal{S}^{22}u_\theta\right) + \frac{1}{r}\left(2\mathcal{S}^{12} + \frac{2}{r}\mathcal{S}^{11}u_{\theta,r} + \frac{2}{r}\mathcal{S}^{13}u_{\theta,z}\right) + \\ &+ \frac{1}{r}\mathcal{S}^{11}u_{\theta,rr} + \frac{2}{r}\mathcal{S}^{13}u_{\theta,rz} + \frac{1}{r}\mathcal{S}^{33}u_{\theta,zz} + \frac{1}{r}\mathcal{S}^{11}_{,r}u_{\theta,r} + \frac{1}{r}(\mathcal{S}^{13})_{,r}u_{\theta,z} + \\ &+ \frac{1}{r}(\mathcal{S}^{13})_{,z}u_{\theta,r} + \frac{1}{r}(\mathcal{S}^{33})_{,z}u_{\theta,z} - \frac{1}{r^2}\mathcal{S}^{11}u_{\theta,r} - \frac{1}{r^2}\mathcal{S}^{13}u_{\theta,z} = \rho\frac{1}{r}\ddot{u}_\theta\end{aligned} \tag{35}$$

The above equation is expressed in two different notations. The stress tensor components are expressed in contravariant coordinates while the displacements and their derivatives are already expressed in cylindrical coordinates. Therefore, the only remaining step is to transform the stress tensor components into cylindrical coordinates. To this effect, the following relationships are used,

$$\mathcal{S}^{11} = \mathcal{S}_{rr}; \quad \mathcal{S}^{22} = \frac{\mathcal{S}_{\theta\theta}}{r^2}; \quad \mathcal{S}^{33} = \mathcal{S}_{zz}; \quad \mathcal{S}^{12} = \frac{\mathcal{S}_{r\theta}}{r}; \quad \mathcal{S}^{13} = \mathcal{S}_{rz}; \quad \mathcal{S}^{23} = \frac{\mathcal{S}_{\theta z}}{r} \tag{36}$$

which, by substitution into Equation 35 yields,

$$\begin{aligned}&\frac{\mathcal{S}_{r\theta,r}}{r} + \frac{1}{r}\mathcal{S}_{\theta z,z} - \frac{1}{r^3}\mathcal{S}_{\theta\theta}u_\theta + \frac{2}{r^2}\mathcal{S}_{r\theta} + \frac{1}{r^2}\mathcal{S}_{rr}u_{\theta,r} + \\ &+ \frac{1}{r}\mathcal{S}_{rr}u_{\theta,rr} + \frac{2}{r}\mathcal{S}_{rz}u_{\theta,rz} + \frac{1}{r}\mathcal{S}_{zz}u_{\theta,zz} + \\ &+ \frac{1}{r}\mathcal{S}_{rr,r}u_{\theta,r} + \frac{1}{r}\mathcal{S}_{rz,z}u_{\theta,r} = \rho\frac{1}{r}\ddot{u}_\theta\end{aligned} \tag{37}$$

The Equation 37 represents the nonlinear torsional wave motion equation expressed in cylindrical coordinates. This new mathematical formulation considers for the first time all the nonlinear terms of the equation associated with finite strains. To obtain the equation in terms of the displacements, it is necessary to calculate $\mathcal{S}$. This final step is achieved by employing the strain energy function.

3.1 Strain energy function

As mentioned in Section 1, hyperelastic materials are those with a strain energy function, $\mathcal{W}$, such that the stress can be calculated as the derivative of the strain energy per unit undeformed volume, such that,

$$\mathcal{S}^{ij} = \frac{\partial \mathcal{W}}{\partial \varepsilon_{ij}} \tag{38}$$

Apart from Landau and Hamilton, several authors, like Rivlin and Ogden, have proposed their own strain energy function [?, ?]. However, the choice of the Hamilton's function is justified due to the quasi-incompressible behavior of the soft tissue, due to their fluid content. In addition, this strain energy function has two additional advantages. First, it has only two non-linear coefficients, which makes it simpler to obtain them by experimental testing. Second, several authors have studied this strain energy function for non-linear waves in incompressible solids with successful results [?].

Hamilton's strain energy function was defined in Equation 5. The constitutive relation, considering the Hamilton's strain energy, is obtained by replacing Equation 5 into the Equation 38, yielding,

$$\mathcal{S}^{ij} = \mu \frac{\partial I_2}{\partial \varepsilon_{ij}} + \frac{1}{3} A \frac{\partial I_3}{\partial \varepsilon_{ij}} + 2 D I_2 \frac{\partial I_2}{\partial \varepsilon_{ij}} \tag{39}$$

where the second and the third invariant are defined in terms of the covariant components of the Green-Lagrange strain tensor as,

$$\begin{aligned} I_2 &= \varepsilon_{im}\varepsilon_{nk}\, g^{ik} g^{nm} = \varepsilon_{11}^2 + 2\varepsilon_{13}^2 + \varepsilon_{33}^2 + 2\frac{\varepsilon_{12}^2}{r^2} + 2\frac{\varepsilon_{23}^2}{r^2} + \frac{\varepsilon_{22}^2}{r^4} \\ I_3 &= \varepsilon_{pm}\varepsilon_{in}\varepsilon_{kq}\, g^{im} g^{pq} g^{kn} = \varepsilon_{11}^3 + 3\varepsilon_{11}\varepsilon_{13}^2 + 3\varepsilon_{13}^2\varepsilon_{33} + \varepsilon_{33}^3 + \frac{3\varepsilon_{11}}{r^2}\varepsilon_{12}^2 + \\ &\quad + \frac{6\varepsilon_{12}}{r^2}\varepsilon_{13}\varepsilon_{23} + \frac{3\varepsilon_{33}}{r^2}\varepsilon_{23}^2 + \frac{3\varepsilon_{22}}{r^4}\varepsilon_{12}^2 + \frac{3\varepsilon_{22}}{r^4}\varepsilon_{23}^2 + \frac{\varepsilon_{22}^3}{r^6} \end{aligned} \tag{40}$$

As ε_{ij} is known, I_2 and I_3 can be determined in terms of the displacements. Equation 39 represents the constitutive relation between the second Piola-Kirchhoff stress tensor and the Green-Lagrange strain tensor. This nonlinear equation is related to the physical nonlinearity. In this manner, both geometrical and physical nonlinearity are here considered.

Finally, as Equation 37 is written in cylindrical coordinates, the constitutive relation (Equation 39) must also be expressed in this system. To this effect, the relationships between contravariant and cylindrical components of $\mathcal{S}$ are used (Equations 36). In Appendix A, the components of $\mathcal{S}$ expressed in the cylindrical coordinate system are detailed. By replacing those components of the stress tensor into the Equation 37, the partial differential equation would be obtained in terms of the displacements.

However, to calculate the close form solution is not possible because the resulting equation is not mathematically treatable at this time. In addition, the boundary conditions of the problem are expressed in a more straightforward manner in terms of velocities and stresses. For these two reasons, Equation 37 is considered to be solved.

4 Numerical results

The difficulty of finding the close form solution makes it necessary to use numerical methods. The variant of the Finite Difference Method, the so-called Finite Difference Time Domain, is used in this study to compute the approximate solution of the problem [?]. This method is detailed in Appendix B.

The problem, depicted in Figure 1a, consists in a nonlinear torsional wave propagating through a tissue-like material from an emitter to a receiver, made with PLA (Polylactic Acid) [?]. As tissue-like material, hydrogel has been considered because its mechanical properties are similar to those of a soft tissue. As the configuration is axilsymmetric, the 3D problem can be solved as a 2D problem (coordinates r and z) what allows reducing the computational cost. Besides, the symmetry of the configuration allows dealing with only half of the problem. To simplify the problem, both spatial dimensions have the same resolution. The spatial resolution ($\Delta r = \Delta z$) is established according to stability conditions. To ensure an adequate representation, 20 elements per wavelength are considered, according to Gomez *et al.* [?],

$$20 \cdot \max\{\Delta r, \Delta z\} < \lambda_{\min} \tag{41}$$

where $\Delta r = \Delta z$ are the spatial resolutions and $\lambda_{\min}$ is the wavelength. A spatial spacing $\Delta r = \Delta z = 50 \cdot 10^{-5}\,\mathrm{m}$ is considered. Once the spatial resolution has been set, the next is to determine the time step. For stability reasons, the Courant-Friedrich-Lewy (CFL) condition is used [?],

$$\max(c_s) \cdot \Delta t < \left[\frac{1}{\Delta r^2} + \frac{1}{\Delta z^2}\right]^{-\frac{1}{2}} \tag{42}$$

where c_s is the shear wave velocity. The temporal resolution is determined: $\Delta t = 2.5 \cdot 10^{-5}\,\mathrm{s}$. The duration of the simulation must be long enough to ensure that all the cycles of the excitation signal are recorded at the receiver. To this effect, a duration of $t_{\mathrm{time}} = 0.01\,\mathrm{s}$ and 400 time steps are considered.

The thickness of the emitter, the hydrogel and the receiver are $t_e = 2.1 \cdot 10^{-3}\,\mathrm{m}$, $t_h = 3.4 \cdot 10^{-3}\,\mathrm{m}$ and $t_{\mathrm{PLA}} = 2 \cdot 10^{-3}\,\mathrm{m}$, respectively. The size of domain at the z and r direction are $zS = 15 \cdot 10^{-3}\,\mathrm{m}$ and $rS = 18 \cdot 10^{-3}\,\mathrm{m}$, respectively. The magnitude rS has been chosen to ensure that the torsional device is not larger than the domain.

The tissue-like hydrogel has the following parameters: density, $\rho = 1000\,\mathrm{kg/m^3}$ and shear stiffness, $\mu = 3610\,\mathrm{Pa}$. With this value of μ, the shear wave velocity is similar to that of soft tissue (1.8 - 2 m/s). The nonlinear parameters A and D have not been experimentally determined for many materials. As there is a lack of information about their values, those calculated by Renier *et al.* for the gelatin are taken as reference [?].

The boundary conditions are expressed in terms of velocities and stresses since the problem is formulated in these variables. Geometrical and mechanical symmetries have

a) b)

Figure 1: a) Representation of the domain where symmetry has been considered and b) boundary conditions of the numerical simulation.

been taken into account. Thus, the symmetry axis (boundary A in Figure 1b) must be fixed, i.e., the velocity is $\dot{u}_\theta = 0$. Along the free boundaries (see boundaries C and E in Figure 1b), the displacements are permitted without any constraint and no stresses are created. In these boundaries the components of the second Piola-Kirchhoff stress tensor are nil. In the contact between the receiver and the hydrogel (boundary D in Figure 1b), experimental results with a high-speed camera using particles on the surface of the hydrogel have proved that these particles remain motionless. Therefore, the velocity is $\dot{u}_\theta = 0$. The propagation of the signal cannot be simulated indefinitely along the space. An issue arises when analyzing open space regions where the simulation domain must be limited. In this case, the boundary conditions, called *Radiation Boundary Conditions* (RBC) or *Absorbing Boundary Conditions* (ABC), are established to simulate the open space. In this work, to ensure that the boundary does not reflect the wave, an ABC has been considered in those boundaries where the stress is equal to zero and the wave can be reflected. [redacted].

Finally, the signal excitation (boundary B in Figure 1b) is implemented. To study the influence of the excitation signal, the tissue will be excited at three different frequencies. These three frequencies are 500 Hz, 1500 Hz and 2000 Hz. To excite the nonlinear terms, it is necessary to repeat the signal for a minimum number of cycles. Experimentally, it has been found that at least six or eight cycles are required to capture nonlinearity. Eight cycles have been considered in this study. In order to simplify the signal, it has been assumed to be sinusoidal.

4.1 Analysis of results

The solution for different excitation frequency values were obtained. Figure 2 shows the displacement u_θ at the contact between the receiver and the hydrogel for the three frequencies. The displacement is calculated as the mean of the displacements recorded at all nodes on the line of contact between the receiver and the hydrogel. These displacements are calculated by multiplying the velocity by the time increment. All the simulations had a computational time of approximately 60 seconds with a 1.7 GHz processor. The linear propagation is also represented for comparison purposes. The linear and the nonlinear solutions have a very similar behavior as the two curves follow the same trend. It can be observed that the curves associated with 500 Hz have very close values to each other and when the frequency of the excitation increases to 1500 Hz, the maximum values of both curves are distanced in the order of 4 μm. When the excitation frequency increases to 2000 Hz the differences decrease again. Therefore, the similarity between the linear and the nonlinear solution increases and decreases in a way that is not proportional to the excitation frequency.

It can be noticed that the nonlinear curve does not have a purely sinusoidal behavior as the linear curve does. Conversely, the ridges and valleys are slightly sloping, which is normal because of its nonlinear nature. The Fast Fourier Transform (FFT) algorithm has been used to obtain the solution in the frequency domain. The main remark about the fr
instar
the fi

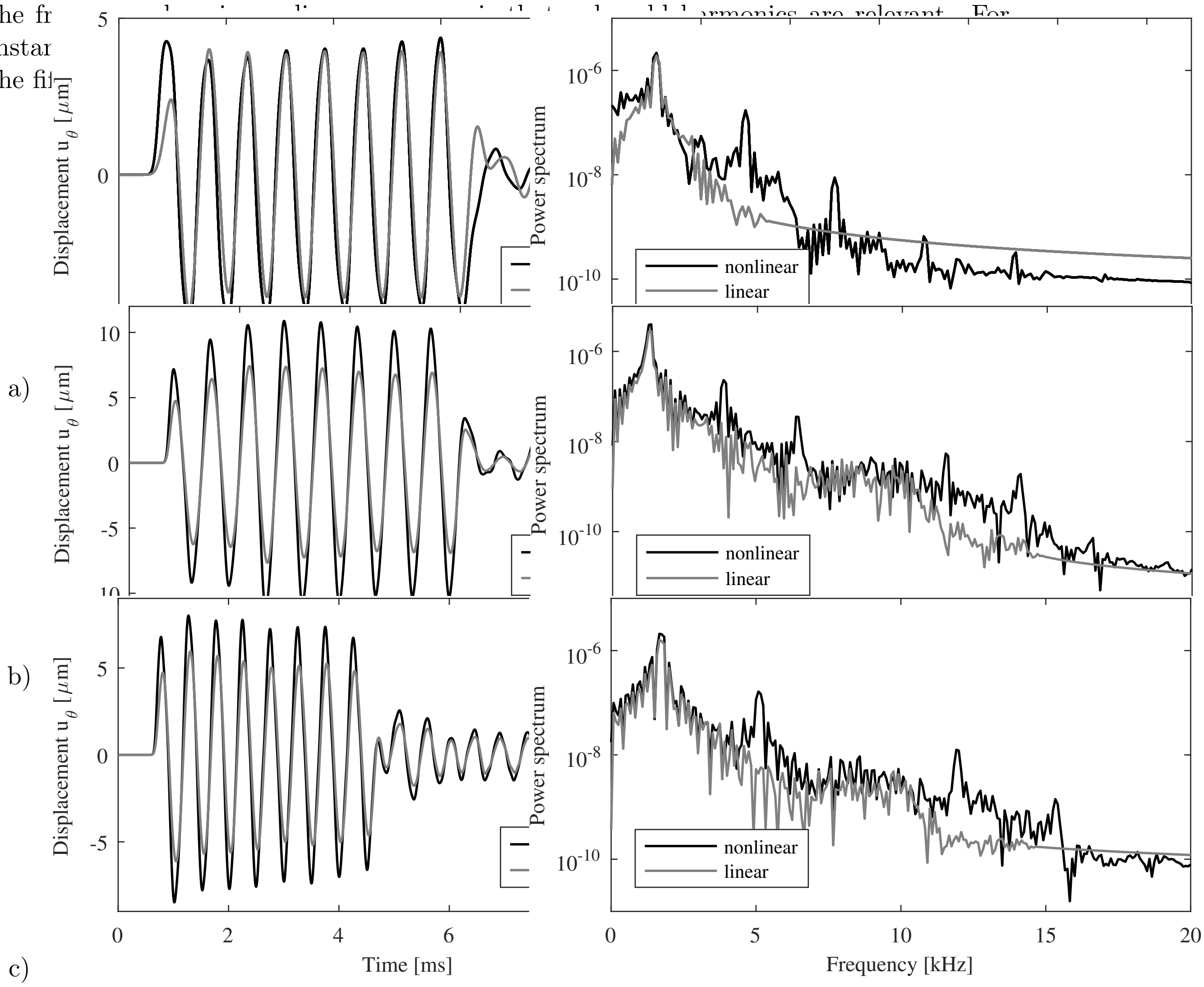

Figure 2: Displacement u_θ at the receiver (left column) and Fourier transform (right column) for a frequency of: a) 500 Hz, b) 1500 Hz and c) 2000 Hz. The parameters of the hydrogel are: $A = 40$ kPa and $D = 3000$ kPa.

With the aim of obtaining the influence of the parameters A and D on the solution,

the nonlinear propagation is represented below for different values of these parameters. For this purpose, the excitation signal considered for all the simulations has a frequency of 2000 Hz. The displacement at the receiver, modifying the value of D and keeping the value of $A = 40\,\mathrm{kPa}$ and $A = 400\,\mathrm{kPa}$, is shown in Figures 3 and 4, respectively. It can be observed that the difference between the linear and nonlinear solution increases significantly as the value of D increases. This difference is due to the higher relevance of the third order nonlinear terms. It is still observed that the nonlinear curve does not exhibit a purely sinusoidal behavior. The frequency domain response shows a similar behavior as their similarity decreases as the value of D increases. Moreover, for the lower valu
bec

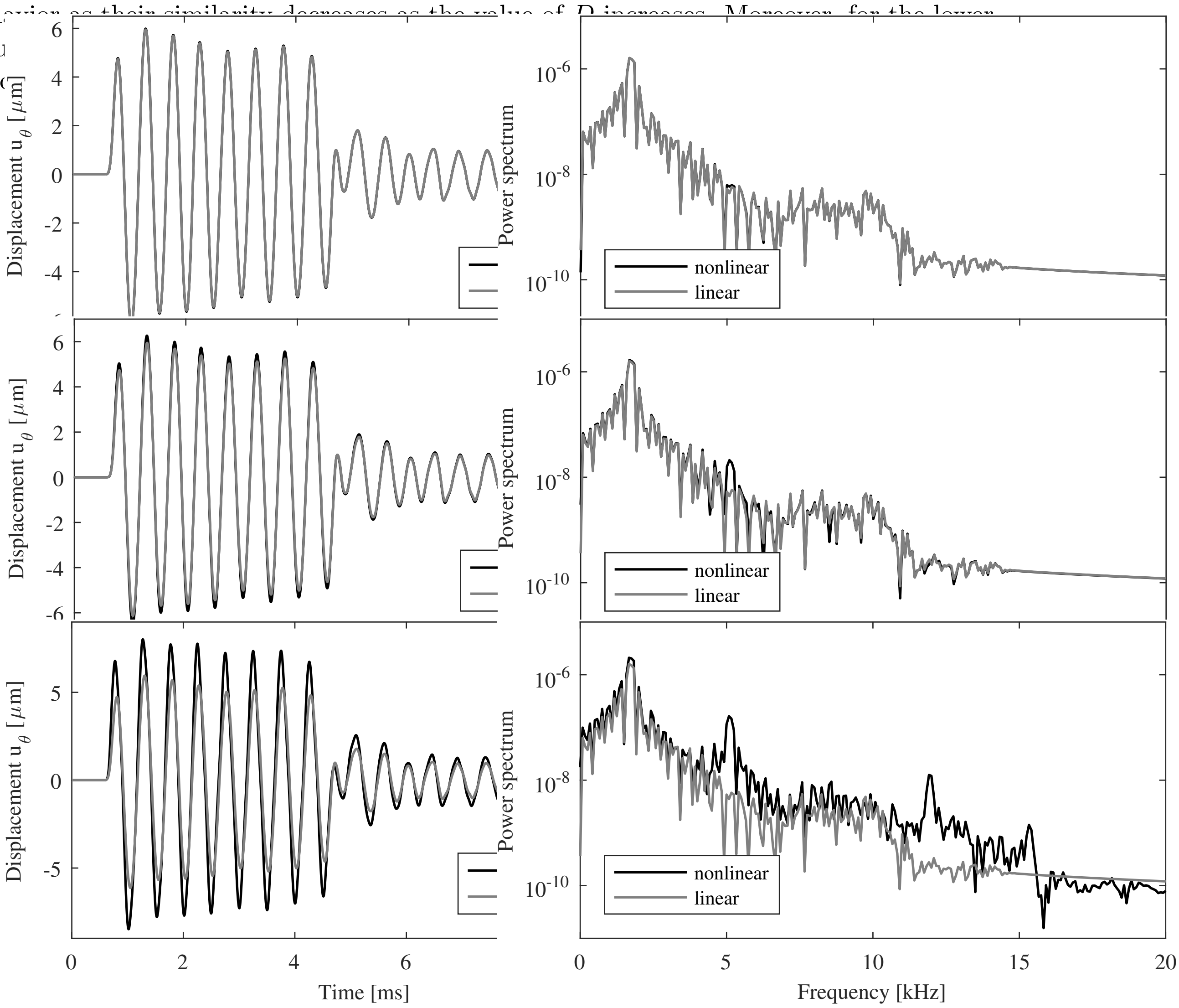

a)

b)

c)

Figure 3: Displacement u_θ at the receiver (left column) and Fourier transform (right column) for a frequency of 2000 Hz. The parameters of the hydrogel are: $A = 40\,\mathrm{kPa}$ and a) $D = 30\,\mathrm{kPa}$, b) $D = 300\,\mathrm{kPa}$ and c) $D = 3000\,\mathrm{kPa}$.

The influence of D in the results is higher as its value increases. Performing a similar procedure keeping the value of D and modifying the value of A conducted to the results in Figure 5. The influence of A is not significant since the solutions for both values of A are very similar.

To analyze the convergence of the solution, the same simulations were carried out dividing the temporal resolution of Equation 42 by two ($1.25 \cdot 10^{-5}$ s) and by four ($6.25 \cdot$

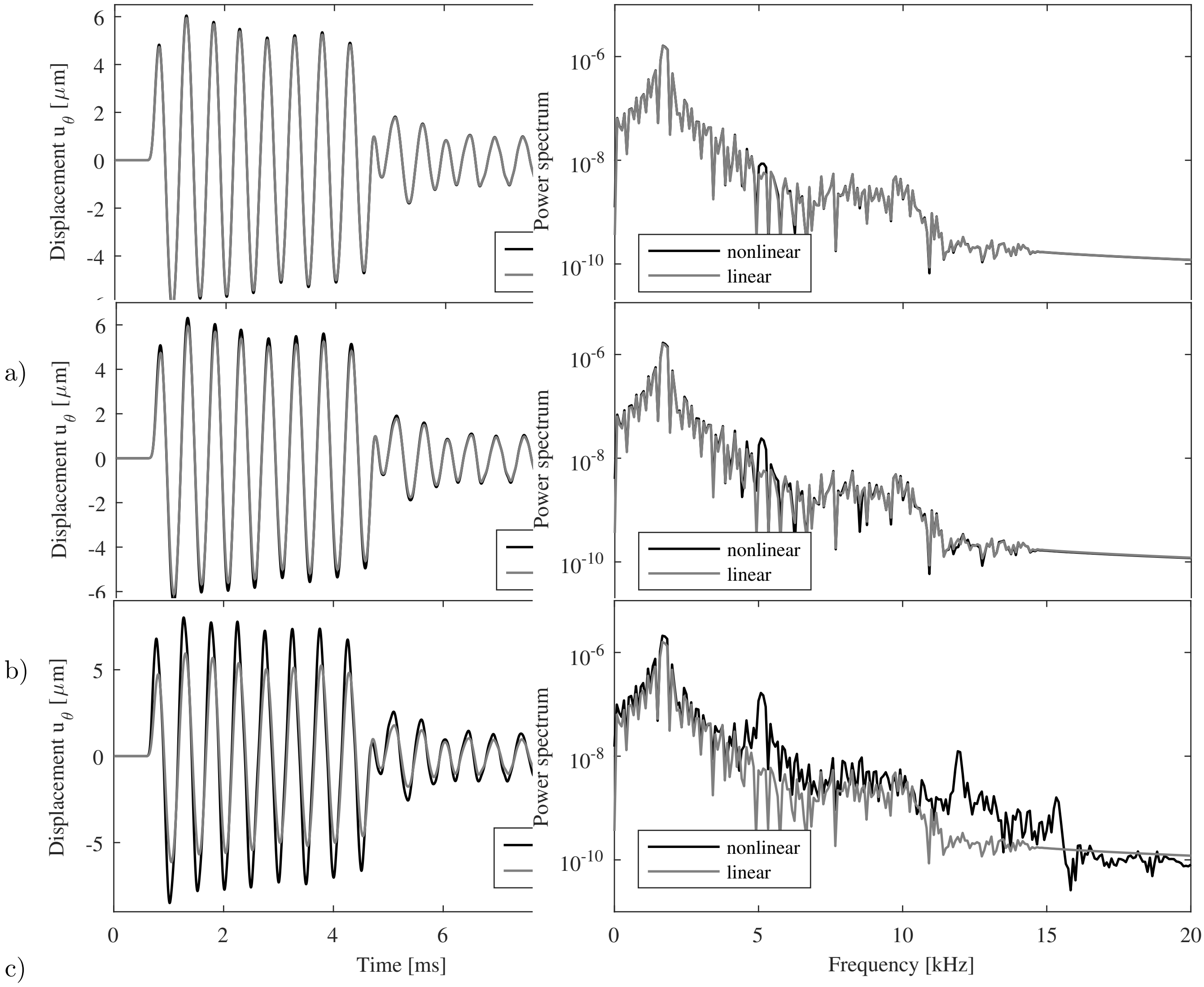

Figure 4: Displacement u_θ at the receiver (left column) and Fourier transform (right column) for a frequency of 2000 Hz. The parameters of the hydrogel are: $A = 400\,\mathrm{kPa}$ and a) $D = 30\,\mathrm{kPa}$, b) $D = 300\,\mathrm{kPa}$ and c) $D = 3000\,\mathrm{kPa}$.

10^{-6} s). The results were not different to the results in Figures 2-5. Hence, the first temporal resolution was small enough both to guarantee the stability of the algorithm and to ensure the convergence of the solution.

[redacted] [?] [redacted] [?] [redacted] [?] [redacted]

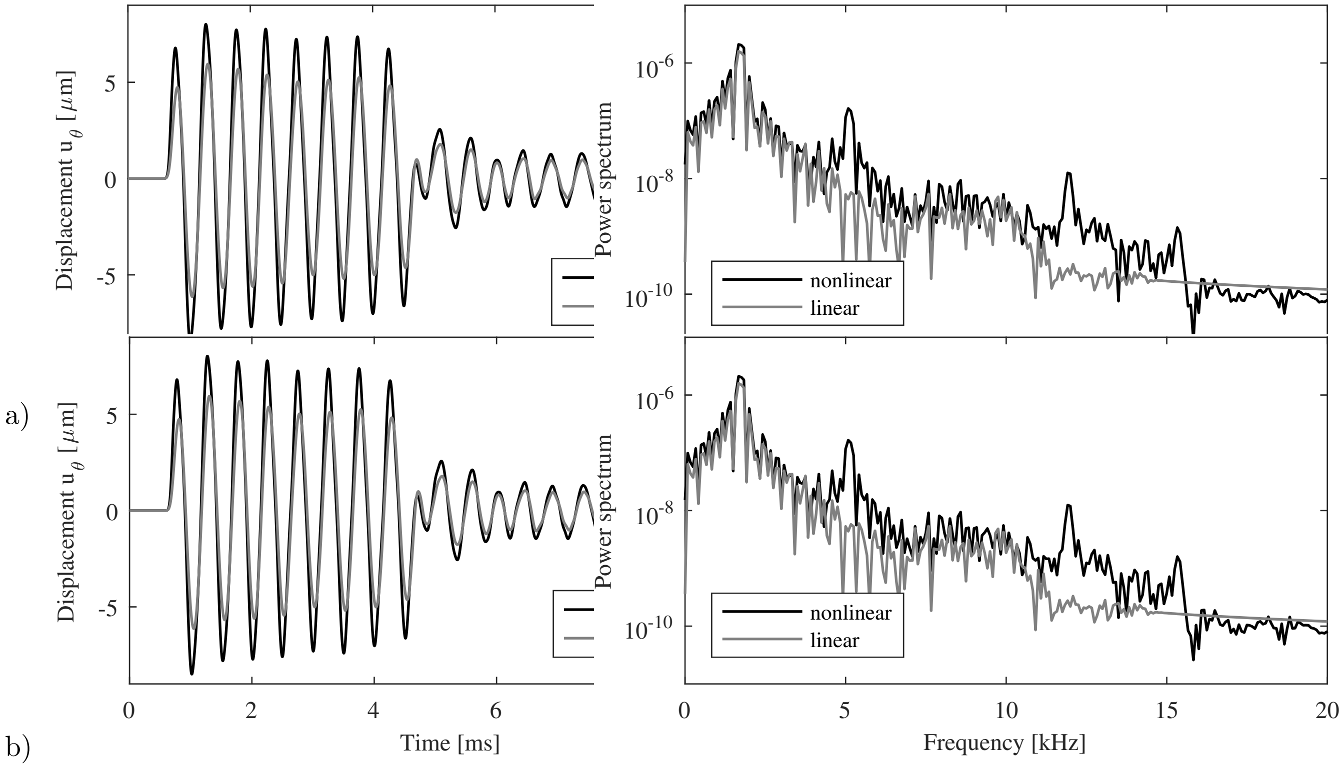

Figure 5: Displacement u_θ at the receiver (left column) and Fourier transform (right column) for a frequency of 2000 Hz. The parameters of the hydrogel are: $D = 3000\,\text{kPa}$ and a) $A = 40\,\text{kPa}$ and b) $A = 400\,\text{kPa}$.

5 Conclusions and future works

The main contribution of this study is the developing of a new formulation in cylindrical coordinates of the propagation of a torsional wave on a hyperelastic material considering the Hamilton's strain energy function. In addition, considering both geometrical and physical nonlinearity, no nonlinear terms of the equation have been neglected. For this reason, a new breakthrough has been achieved in the field of mechanical modeling of soft tissues since, until now, there have been no analytical motion equations in cylindrical coordinates using Hamilton's strain energy function.

Due to the difficulty of obtaining the close form solution, a numerical simulation of a torsional wave propagating along a hydrogel from an emitter to a receiver has been conducted. The numerical solution has been derived by implementing the Finite Difference Time Domain algorithm. The analysis of results has led to some concluding remarks. First, when the nonlinear parameters of the material remain constant, the similarity between the linear and nonlinear solution decreases with the increase of the excitation frequency. Second, for a given excitation frequency, the behavior of both curves is less similar with the increase of the value of the parameter D. However, the value of the parameter A seems to be not significant since its variation does not affect the solution of the simulations performed. Therefore, the parameter D has been proved to have a larger influence on the behavior of the tissue-like material.

The formulation presented in this study allows determining the strain that a material medium will suffer when a torsional wave propagates through it. An advantage is the use of a torsional wave instead of compressional and shear waves. The former is more sensitive to consistency changes because it is generated in a low energy regime. In addition, by employing a torsional wave device, experimental tests could be performed on tissues to measure the strain level caused by the nonlinear torsional wave. These results can be used to solve a parameter identification problem by means of an inverse problem. As a result, the parameter values that minimize the numerical and experimental results of medical applications are obtained. In this way, the nonlinear parameters of the material can be derived. The knowledge of nonlinear parameters would provide information on the current state of the tissue and allow a clinical diagnosis to be conducted.

Acknowledgements

This research was supported by the Ministry of Education DPI2014-51870-R, and UNGR15-CE-3664, Ministry of Health DTS15/00093 and PI16/00339 Carlos III/FEDER, and Junta de Andalucía P11-CTS-8089, PI-0107-2017, PIN-0030-2017 and UGR PP2017-PIP2019 projects.

A Cylindrical components of stress tensor

In this appendix, the second Piola-Kirchhoff stress tensor components expressed in the cylindrical coordinate system are presented. By substituting these expressions into Equation 37, the motion equation would be derived in terms of the displacements.

$$
\begin{aligned}
\mathcal{S}_{rr} = \mathcal{S}^{11} =& \mu u_{\theta,r}^2 + \frac{1}{4} A \left(\frac{\left(r u_{\theta,r} - u_\theta \right)^2}{r^2} + u_{\theta,r}^4 + u_{\theta,z}^2 u_{\theta,r}^2 \right) + \\
& + \frac{1}{2} D \left(2u_{\theta,z}^2 + \frac{u_\theta^4}{r^4} + \frac{2\left(r u_{\theta,r} - u_\theta \right)^2}{r^2} + u_{\theta,z}^4 + u_{\theta,r}^4 + 2u_{\theta,z}^2 u_{\theta,r}^2 \right) u_{\theta,r}^2
\end{aligned}
\tag{43}
$$

$$
\begin{aligned}
\mathcal{S}_{\theta\theta} = r^2 \mathcal{S}^{22} =& \mu \frac{u_\theta^2}{r^2} + \frac{1}{4} A \left(u_{\theta,z}^2 + \frac{u_\theta^4}{r^4} + \frac{\left(r u_{\theta,r} - u_\theta \right)^2}{r^2} \right) + \\
& + \frac{1}{2r^2} D \left(2u_{\theta,z}^2 + \frac{u_\theta^4}{r^4} + \frac{2\left(r u_{\theta,r} - u_\theta \right)^2}{r^2} + u_{\theta,z}^4 + u_{\theta,r}^4 + 2u_{\theta,z}^2 u_{\theta,r}^2 \right) u_\theta^2
\end{aligned}
\tag{44}
$$

$$
\begin{aligned}
\mathcal{S}_{zz} = \mathcal{S}^{33} =& \mu u_{\theta,z}^2 + \frac{1}{4} A \left(u_{\theta,z}^2 + u_{\theta,z}^4 + u_{\theta,r}^2 u_{\theta,z}^2 \right) + \\
& + \frac{1}{2} D \left(2u_{\theta,z}^2 + \frac{u_\theta^4}{r^4} + \frac{2\left(r u_{\theta,r} - u_\theta \right)^2}{r^2} + u_{\theta,z}^4 + u_{\theta,r}^4 + 2u_{\theta,z}^2 u_{\theta,r}^2 \right) u_{\theta,z}^2
\end{aligned}
\tag{45}
$$

$$
\begin{aligned}
\mathcal{S}_{r\theta} = r \mathcal{S}^{12} =& \mu \frac{\left(r u_{\theta,r} - u_\theta \right)}{r} + \frac{A}{4} \left(u_{\theta,r}^3 - \frac{1}{r^3} u_\theta^3 - \frac{1}{r} u_{\theta,r}^2 u_\theta + \frac{1}{r^2} u_\theta^2 u_{\theta,r} + u_{\theta,r} u_{\theta,z}^2 \right) + \\
& + \frac{D}{2r} \left(2u_{\theta,z}^2 + \frac{u_\theta^4}{r^4} + \frac{2\left(r u_{\theta,r} - u_\theta \right)^2}{r^2} + u_{\theta,z}^4 + u_{\theta,r}^4 + 2u_{\theta,z}^2 u_{\theta,r}^2 \right) \left(r u_{\theta,r} - u_\theta \right)
\end{aligned}
\tag{46}
$$

$$
\begin{aligned}
\mathcal{S}_{rz} = \mathcal{S}^{13} =& \mu u_{\theta,z} u_{\theta,r} + \frac{D}{2} u_{\theta,z} \left(2u_{\theta,z}^2 + \frac{u_\theta^4}{r^4} + \frac{2\left(r u_{\theta,r} - u_\theta\right)^2}{r^2} + u_{\theta,z}^4 + u_{\theta,r}^4 + 2u_{\theta,z}^2 u_{\theta,r}^2 \right) u_{\theta,r} + \\
&+ \frac{A}{4} \left(u_{\theta,r}^3 u_{\theta,z} + u_{\theta,z}^3 u_{\theta,r} + u_{\theta,r} u_{\theta,z} - \frac{1}{r} u_\theta u_{\theta,z} \right)
\end{aligned}
\tag{47}
$$

$$
\begin{aligned}
\mathcal{S}_{\theta z} = r\mathcal{S}^{23} =& \mu u_{\theta,z} + \frac{1}{2} D \left(2u_{\theta,z}^2 + \frac{u_\theta^4}{r^4} + \frac{2\left(r u_{\theta,r} - u_\theta\right)^2}{r^2} + u_{\theta,z}^4 + u_{\theta,r}^4 + 2u_{\theta,z}^2 u_{\theta,r}^2 \right) u_{\theta,z} + \\
&+ \frac{A}{4} \left(u_{\theta,z}^3 + u_{\theta,r}^2 u_{\theta,z} - \frac{1}{r} u_{\theta,z} u_{\theta,r} u_\theta + \frac{1}{r^2} u_\theta^2 u_{\theta,z} \right)
\end{aligned}
\tag{48}
$$

B FDTD Method

To solve the problem by using the FDTD method, we must follow several steps. First, Equation 37 must be rewritten in terms of the velocity instead of the acceleration,

$$
\begin{aligned}
&\frac{\mathcal{S}_{r\theta,r}}{r} + \frac{1}{r}\mathcal{S}_{\theta z,z} - \frac{1}{r^3}\mathcal{S}_{\theta\theta} u_\theta + \frac{2}{r^2}\mathcal{S}_{r\theta} + \frac{1}{r^2}\mathcal{S}_{rr} u_{\theta,r} + \\
&+ \frac{1}{r}\mathcal{S}_{rr} u_{\theta,rr} + \frac{2}{r}\mathcal{S}_{rz} u_{\theta,rz} + \frac{1}{r}\mathcal{S}_{zz} u_{\theta,zz} + \\
&+ \frac{1}{r}\mathcal{S}_{rr,r} u_{\theta,r} + \frac{1}{r}\mathcal{S}_{rz,z} u_{\theta,r} = \rho \frac{1}{r}\frac{\mathrm{d}\dot{u}_\theta}{\mathrm{d}t}
\end{aligned}
\tag{49}
$$

Recalling that the FDTD method calculates the derivatives as differences, the time differential $\mathrm{d}t$ becomes an increment Δt. Therefore, the velocity $\dot{u}_\theta$ can be calculated as,

$$
\begin{aligned}
\dot{u}_\theta = \frac{\Delta t \cdot r}{\rho} \Bigg[& \frac{\mathcal{S}_{r\theta,r}}{r} + \frac{1}{r}\mathcal{S}_{\theta z,z} - \frac{1}{r^3}\mathcal{S}_{\theta\theta} u_\theta + \frac{2}{r^2}\mathcal{S}_{r\theta} + \frac{1}{r^2}\mathcal{S}_{rr} u_{\theta,r} + \\
+ & \frac{1}{r}\mathcal{S}_{rr} u_{\theta,rr} + \frac{2}{r}\mathcal{S}_{rz} u_{\theta,rz} + \frac{1}{r}\mathcal{S}_{zz} u_{\theta,zz} + \frac{1}{r}\mathcal{S}_{rr,r} u_{\theta,r} + \frac{1}{r}\mathcal{S}_{rz,z} u_{\theta,r} \Bigg]
\end{aligned}
\tag{50}
$$

Considering the Taylor series expansion of a function $f(x)$ expanded about the point x_0 with an offset of $\pm\delta/2$, following the procedure described in many test books such us [?], the central difference approximation is,

$$
f'(x_0) \approx \frac{f\left(x_0 + \frac{\delta}{2}\right) - f\left(x_0 - \frac{\delta}{2}\right)}{\delta} \tag{51}
$$

where it has been assumed that δ is sufficiently small and higher order terms can be neglected.

By considering an offset of $\pm\delta$ for the second derivative, the same procedure yields,

$$
f''(x_0) \approx \frac{f\left(x_0 + \delta\right) - 2f(x_0) + f\left(x_0 - \delta\right)}{\delta^2} \tag{52}
$$

Spatial derivatives in Equation 50 are calculated using Equations 51 and 52. The expressions of the derivatives are given below,

$$
\begin{aligned}
\mathcal{S}_{r\theta,r} &= \frac{\mathcal{S}_{r\theta}(r_0+\Delta r)-\mathcal{S}_{r\theta}(r_0)}{\Delta r}\\
\mathcal{S}_{\theta z,z} &= \frac{\mathcal{S}_{\theta z}(z_0+\Delta z)-\mathcal{S}_{\theta z}(z_0)}{\Delta z}\\
\mathcal{S}_{rr,r} &= \frac{\mathcal{S}_{rr}(r_0+\Delta r)-\mathcal{S}_{rr}(r_0)}{\Delta r}\\
\mathcal{S}_{rz,z} &= \frac{\mathcal{S}_{rz}(z_0+\Delta z)-\mathcal{S}_{rz}(z_0)}{\Delta z}\\
u_{\theta,r} &= \frac{u_\theta(r_0+\Delta r)-u_\theta(r_0)}{\Delta r}\\
u_{\theta,rr} &= \frac{u_\theta(r_0+\Delta r)-2u_\theta(r_0)+u_\theta(r_0-\Delta r)}{\Delta r^2}\\
u_{\theta,zz} &= \frac{u_\theta(z_0+\Delta z)-2u_\theta(z_0)+u_\theta(z_0-\Delta z)}{\Delta z^2}\\
u_{\theta,rz} &= \frac{u_\theta(z_0+\Delta z,r_0+\Delta r)+u_\theta(r_0,z_0)-u_\theta(z_0,r_0+\Delta r)-u_\theta(z_0+\Delta z,r_0)}{\Delta r\Delta z}
\end{aligned}
$$

The next step is to obtain the relation between the components of the second Piola-Kirchhoff Stress Tensor and the velocity $\dot{u}_\theta$ by differentiating them with respect to the time,

$$\frac{\mathrm{d}\mathcal{S}(u_\theta)}{\mathrm{d}t} = \mathcal{S}(u_\theta,\dot{u}_\theta) \tag{53}$$